The effect of temperature variations on the camber of precast, prestressed concrete girders

Hang Nguyen, John Stanton, Marc Eberhard, and David Chapman

- Field measurements of daily variations in temperature profile and camber for two precast, prestressed concrete girders provided data with which to calibrate models of the effect of temperature variations on camber.

- Camber history was computed using measured temperature profiles and an assumed coefficient of thermal expansion of $5.5 \times 10^{-6}/°F$ ($9.9 \times 10^{-6}/°C$).

- Two practical methods were also developed using 164 observations from 24 girders.

Most medium-span bridges in the United States are constructed with precast, prestressed concrete girders that support a cast-in-place concrete deck. These girders usually have an upward deflection (camber) that results from the combined effects of the eccentric axial prestressing force and the gravity loads. If the camber is less than expected, the contractor must increase the amount of concrete needed to construct the cast-in-place concrete pad between the top of the girder and the deck. If the camber is greater than expected, the girder may interfere with placement of the deck reinforcement. Differences between expected and actual cambers are even more critical if the bridge owner rejects the girder for being out of compliance with the specifications.

The prediction of girder camber at a particular time is difficult because it depends on the concrete properties, curing conditions, prestress losses, and temperature variations within the girder, all of which vary with time.[1,2] One contributor to this difficulty is the effect of variations in the profile of internal temperatures over a day. Such variations induce thermal strains, which, if they vary over the height of the girder, result in camber even in the absence of external loads.

Thermal camber typically has the most important consequences during construction. At that time, the girders are

statically determinate, so no bending moments exist to restrain the camber, which is therefore at a maximum. If the girders are later connected longitudinally to create a continuous system, any thermally induced camber induces continuity moments, which reduce the magnitude of the thermal camber for a given temperature gradient. The addition of the cast-in-place concrete deck also tends to reduce camber.

This paper investigates the effects on camber of variations of temperature over the height of the girder before a slab is cast. After discussing previous work in this area, the paper describes the experimental program, which included monitoring of camber and temperatures. The time-dependent, measured internal temperature profiles were used to generate theoretical camber histories, which were compared with the measured values. The paper then develops two new, practical methods that allow the designer to estimate the expected camber in a bridge girder due to diurnal temperature variations. Camber variations arise from multiple causes, which are too numerous and complex to evaluate in a single paper. This paper addresses only cambers induced by thermal gradients.

The methods proposed herein may be used for estimating thermal camber for a known temperature environment. Knowledge of the thermal camber is expected to be helpful for making appropriate elevation allowances when setting formwork for the cast-in-place deck slab, for estimating the additional concrete required in the haunch over the girder, and, in extreme cases, for ensuring that girders are not rejected for having camber that lies outside the specified range.

Previous work

For the purpose of design, the American Association of State Highway and Transportation Officials' *AASHTO LRFD Bridge Design Specifications*[3] provide four temperature gradients corresponding to four solar radiation zones in the United States. The gradient depends on the location of the bridge girder, the superstructure depth, and the materials in the superstructure.

The AASHTO LRFD specifications' design gradients are similar in principle to those proposed by Priestley.[4] He studied seven bridge girder sections under the effects of wind, ambient temperature variations, blacktop (asphalt) thickness, and solar absorptivity. For design, he proposed the following vertical temperature profile at the top of the girder:

$$t(Y) = T\left(\frac{Y}{Y_0}\right)^5 \qquad (1)$$

where

$t(Y)$ = change in temperature at height Y

Y = vertical coordinate, measured upwards from a point located Y_0 below the concrete deck surface

Y_0 = distance from top surface at which temperature change is zero, value = 1200 mm = 47.25 in.

T = temperature at top surface of deck

= $32 - 0.2h_a$ (°C) for h_a in mm

= $89.6 - 5.08h_a$ (°F) for h_a in in.

h_a = asphalt thickness

Figure 1 compares the design positive temperature gradient from Eq. (1) with the one recommended by the AASHTO LRFD specifications for a typical large girder.[3] These specifications define a dimension A that controls the depth to which the temperature change penetrates (Fig. 1). The value of A varies with the superstructure depth and materials, and it is 12 in. (300 mm) for concrete superstructures that are at least 16 in. (410 mm) deep. The change in bottom temperature ΔT_3 is 0 unless a site specific study has determined another appropriate value, but it is not to exceed 5°F (3°C). An increase in bottom temperature reduces the thermal camber. A negative design temperature gradient is obtained by multiplying the positive gradient by a factor of -0.2 and -0.3, respectively, for decks with and without asphalt overlays.

A number of researchers have measured temperature gradients and their effects on camber in bridge girders and decks. For example, Shushkewich acquired large amounts of thermocouple data from an instrumented prestressed concrete box girder bridge, the North Halawa Valley Viaduct in Hawaii.[5] The results validated the positive and negative thermal gradients included in the AASHTO LRFD specifications.[3]

Barr monitored changes in camber of five simply supported I-girders during a day to evaluate the bridge's response to daily temperature variations.[6] He found that the camber varied by 0.63 in. (16 mm) between 9:00 a.m. and 9:00 p.m. in one day. He also found that the calculated tensile stresses at the bottom of the girder were larger for the temperature gradient proposed by Priestley than for any of the gradients recommended by the 1994 AASHTO LRFD specifications.[4,7]

Hinkle observed that the cambers of three girders with an average length of 128 ft (39.0 m) varied by up to 0.50 in. (13 mm) between 7:45 a.m. and 1:25 p.m. in the same day.[8] French and O'Neill monitored variations of camber
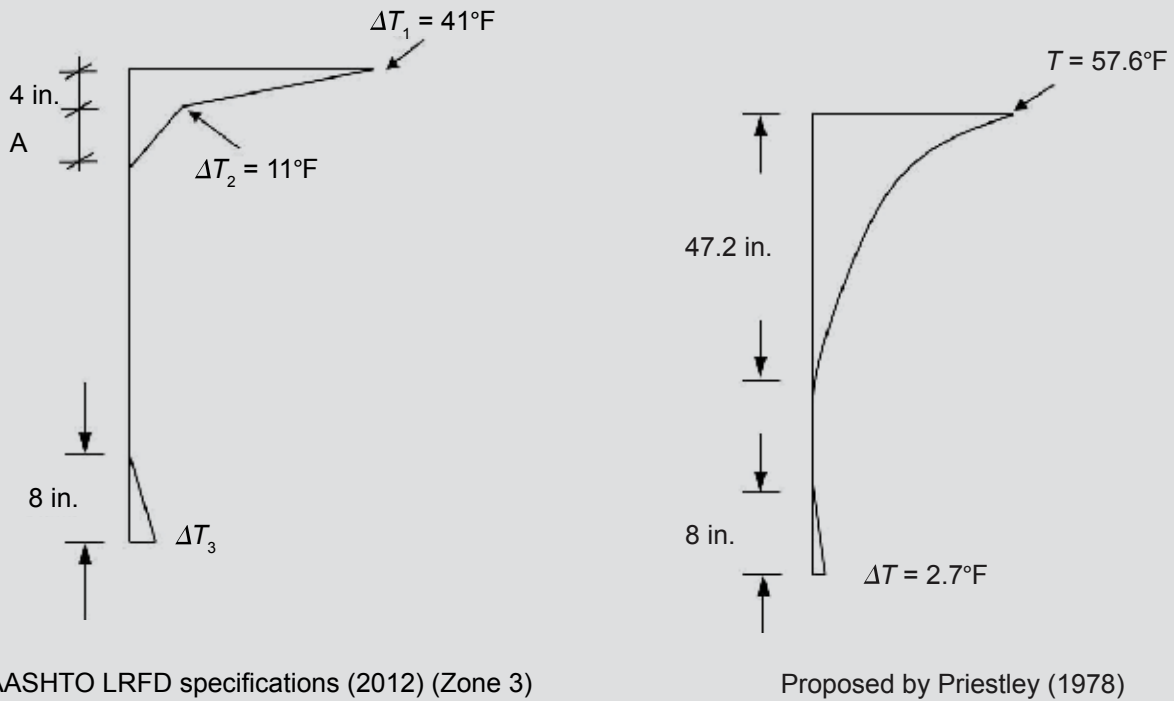
Figure 1. Design temperature gradient. T = temperature at top surface of deck; ΔT = temperature difference over height of girder; ΔT_1 = temperature change at top surface of girder; ΔT_2 = temperature change 4 in. below top surface of girder; ΔT_3 = temperature change at bottom of girder. 1 in. = 25.4 mm; °C = (°F − 32)/1.8.

of 11 girders.[9] Three of these girders were monitored on two separate days, resulting in a total of 14 girder-observation days. The camber of the monitored girders varied during each day by 0.70 to 0.95 in. (18 to 24 mm) for girders ranging in length from 119 to 132 ft (36.3 to 40.2 m). These field observations are used later in this paper to calibrate the proposed simple methods for estimating thermal camber.

Experimental program

In this study, two large prestressed concrete girders were instrumented to quantify daily temperature variations, develop an understanding of the effects of these variations on camber, and calibrate theoretical and more practical models for predicting thermal camber. The results are summarized here. Nguyen gives details.[10]

Table 1 lists key properties for the monitored girders. Both girders were Washington State WF100G girders with an I-shaped cross section and a depth of 100 in. (2500 mm) (appendix 5.6-A4-10, Washington State Department of Transportation *Bridge Design Manual (LRFD)*).[11] Weekday

girders are typically cast at approximately noon on one day and released the next morning. Weekend girders are typically cast on a Friday and released on the following Monday morning. Typically, the concrete for these weekend girders is more mature at release, even though the curing temperature may have been lower, on average, than for a weekday girder. All of the measurements discussed in this paper were taken approximately two months after the prestressing force had been applied to the girder concrete, by which time the effects of creep, shrinkage, and relaxation were expected to be constant over the course of any one day.

The internal temperatures of the two girders were measured at a single cross section near midspan at one-minute intervals using fifteen type J thermocouples. The changes in camber at midspan of the two girders were measured continuously with a deflection sensor in the fabricator's storage yard. **Figure 2** shows the locations of the thermocouples. More thermocouples were placed in the top flange than in the web, both because the top flange was expected to experience the largest variation in temperature during the day and because the thin flange tips had the largest surface/volume ratio, which increases

Table 1. Girder properties							
Girder	**Girder mark**	**Cast date**	**Measurement date**	**Depth, in.**	**Length, ft**	f_c' **at release, psi**	f_c' **at 28 days, psi**
Weekend girder	H6B	May 18, 2012	July 26, 2012	100	172.7	9215	11,260
Weekday girder	H8A	May 29, 2012	July 25 and 26, 2012	100	164.0	8250	12,430

Note: f_c' = compressive strength of concrete. 1 in. = 25.4 mm; 1 ft = 0.305 m; 1 psi = 6.895 kPa.
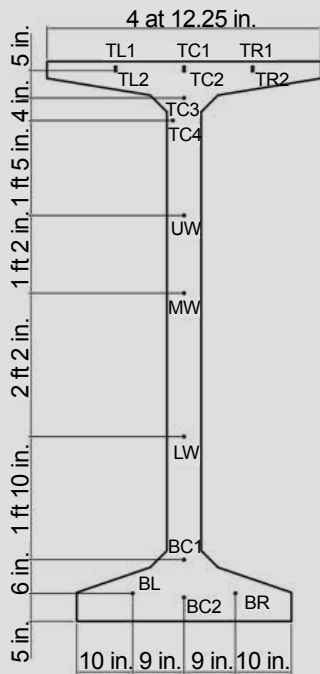
Figure 2. Thermocouple locations. Note: B = bottom of girder; C = center of girder; L = left side of girder; LW = lower web; R = right side of girder; T = top of girder; UW = upper web.

the possibility of transverse (as well as vertical) variations in temperature.

Measured temperature histories

Figure 3 shows the measured internal temperature histories for girder H8A for 22 hours and for girder H6B for 9 hours. A problem with electrical power supply prevented the data logger from monitoring girder H6B for a longer time.

The data follow expected trends. For both girders, the temperature profile over the height of girders was nearly uniform until about 10:00 a.m. During the late morning and afternoon, the temperature in the top of the flange exposed directly to sunlight increased rapidly until it reached a peak at about 4:00 p.m. At this time, the temperature change in the top flange was approximately equal to 40°F (22°C). In contrast, the temperatures in the web and bottom flange changed less because these locations were shaded by the top flange and by adjacent girders in the storage yard. This situation is similar to that which a girder would experience during installation, at which time the flange, adjacent girders, and deck formwork would similarly shadow the web and bottom flange.

The left side of the web of girder H6B was also exposed to direct sunlight, which might be similar to the exposure condition for an exterior girder in a bridge. **Figure 3** plots that exposure data, in which the temperature during the

day, when sunlight was strongest, was higher at the bottom left sensor than at the bottom right or bottom center sensor locations.

In the late afternoon, the internal temperatures in the top of the girder dropped rapidly as the solar radiation became weaker and the air temperature decreased, whereas the temperatures in the web and bottom portions in the girders cooled more slowly. This difference can be explained by the fact that the bottom region of the girders was affected by heat from the ground and was less exposed to wind. During the day, the ground was heated by the sun. However, the ground changes temperature more slowly than does the air, so the bottom flange continued to warm in the evening due to heat from the ground.

Figure 4 shows the corresponding vertical temperature profiles of the girders at various times. For each elevation that had more than one thermocouple (for example, the flanges), the average temperature is plotted at that elevation. The temperatures varied most over the height of the girder at approximately 4:00 p.m.

Calculation of thermal camber changes from temperature profiles

Thermal camber can be predicted from the measured internal temperature profile using the principles of mechanics and an assumed value of the coefficient of thermal expansion. The total strain at any point will consist of
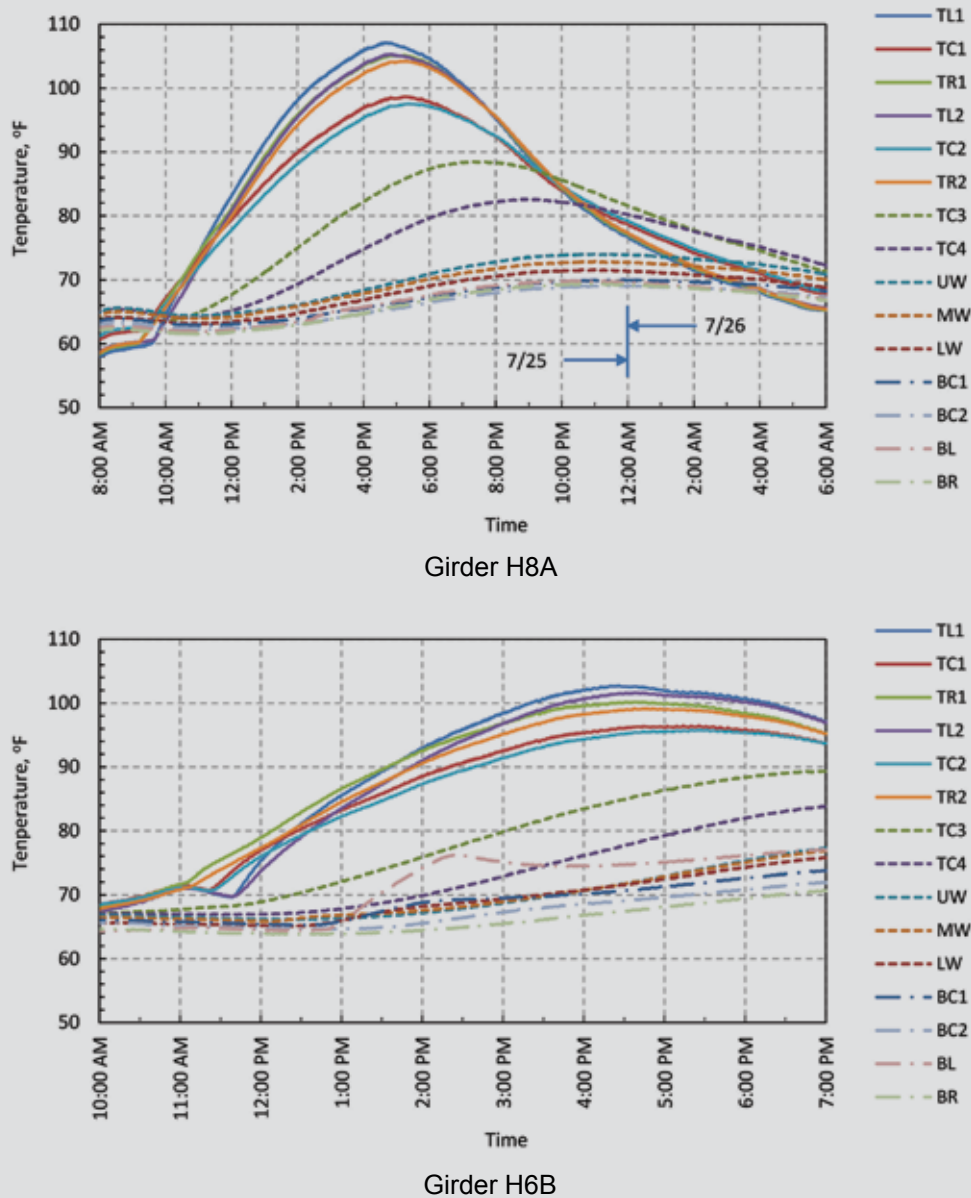
Figure 3. Internal temperature histories. Note: B = bottom of girder; C = center of girder; L = left side of girder; LW = lower web; R = right side of girder; T = top of girder; UW = upper web. °C = (°F − 32)/1.8.

a thermal and a stress-related component (**Fig. 5**). The curvature at each point along the girder can be computed by finding the profile of total strain that satisfies the following assumptions:

- Plane sections remain plane.

- The free thermal strain is constant across the width at any elevation.

- The concrete and steel are within their linear elastic ranges, and the concrete is uncracked.

- The changes in axial force and bending moment due to thermal effects are both zero for the simply supported girder.

Stresses will develop over the depth of the member if the thermal strain gradient is nonlinear. The total strain ε_{tot} is the sum of the free environmental strain ε_e, which consists here of just the thermal strain but more generally may also include other components, such as shrinkage, plus the mechanical strain ε_m, which is given by stress σ divided by Young's modulus E:

$$\varepsilon_{tot} = \varepsilon_e + \varepsilon_m = \varepsilon_e + \sigma / E \qquad (2)$$

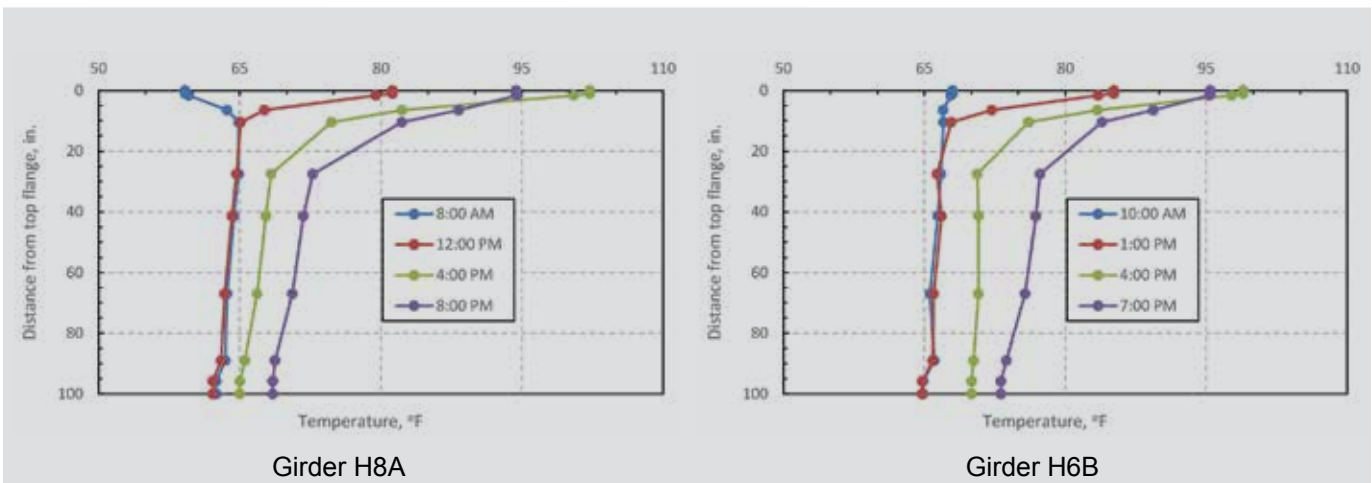If plane sections remain plane, the total strain field must be linear.

Figure 4. Temperature profiles over height of girders. Note: 1 in. = 25.4 mm; ˚C = (˚F − 32)/1.8.
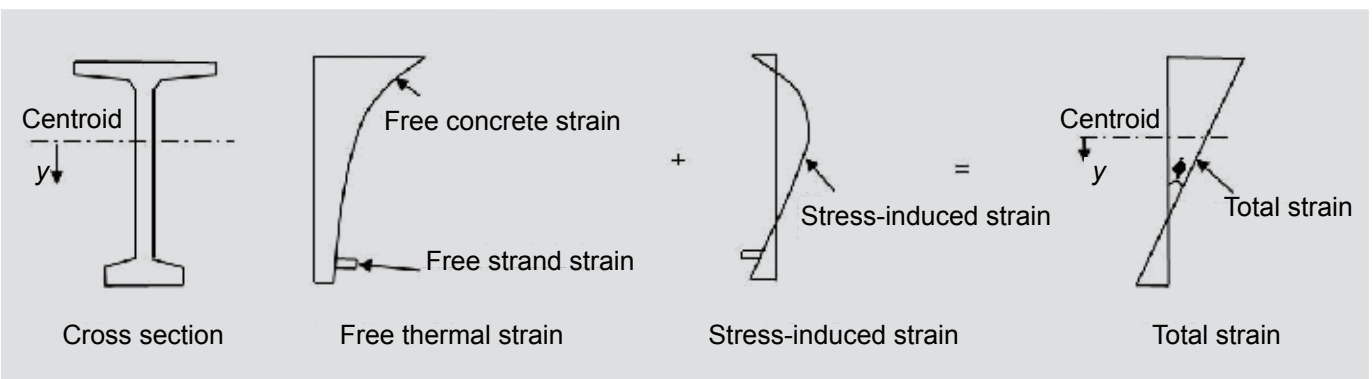

Figure 5. Strain profile in simply supported girder.

$$\varepsilon_{tot} = \varepsilon_0 + \phi y \qquad (3)$$

where

ε_0 = total strain at the origin

ϕ = curvature

y = vertical coordinate, measured positive downwards from the origin

For this derivation, strains are assumed to be positive in tension, and a positive curvature causes downward deflection. The origin may be taken anywhere. Combining Eq. (2) and (3) gives Eq. (4).

$$\sigma = E(\varepsilon_0 + \phi y - \varepsilon_e) \qquad (4)$$

For a statically determinate girder, axial-force equilibrium is determined by Eq. (5).

$$0 = \int \sigma dA = \int E(\varepsilon_0 + \phi y - \varepsilon_e)dA \qquad (5)$$

If the section contains several materials with different properties, they must be taken into account when the integral is evaluated. The two unknowns are ε_0 and ϕ. The integral can be broken into components, and the axial force equilibrium equation can be rearranged to give a linear equation in ε_0 and ϕ (Eq. [6]).

$$\varepsilon_0 \int E dA + \phi \int E y dA = \int E \varepsilon_e dA \qquad (6)$$

Similarly, moment equilibrium at the section requires Eq. (7).

$$0 = \int y \sigma dA = \int y E(\varepsilon_0 + \phi y - \varepsilon_e)dA \qquad (7)$$

Again this equation can be rearranged to give Eq. (8).

$$\varepsilon_0 \int Ey\,dA + \phi \int Ey^2\,dA = \int Ey\varepsilon_e\,dA \qquad (8)$$

These equations can be combined to give Eq. (9).

$$\begin{bmatrix} \int E\,dA & \int Ey\,dA \\ \int Ey\,dA & \int Ey^2\,dA \end{bmatrix} \begin{Bmatrix} \varepsilon_0 \\ \phi \end{Bmatrix} = \begin{Bmatrix} \int E\varepsilon_e\,dA \\ \int Ey\varepsilon_e\,dA \end{Bmatrix} \qquad (9)$$

If the origin is taken as the centroid of the section, the term $\int Ey\,dA$ is, by definition, equal to zero and Eq. (10) and (11) result.

$$\int E\,dA = EA_{tr} \qquad (10)$$

$$\int Ey^2\,dA = EI_{tr} \qquad (11)$$

where

A_{tr} = area of the transformed section

I_{tr} = moment of inertia of the transformed section

If different materials are involved, the centroid is that of the transformed section. The matrix equations decouple to give Eq. (12) and (13).

$$\varepsilon_0 EA_{tr} = \int E\varepsilon_e b(y)\,dy \qquad (12)$$

$$\phi EI_{tr} = \int Ey\varepsilon_e b(y)\,dy \qquad (13)$$

The integrals on the right side of Eq. (12) and (13) are most conveniently evaluated numerically because in most cases the girder width $b(y)$ cannot be defined with a single equation.

The calculations simplify in two special cases. First, if E is the same throughout the girder cross section, Eq. (12) and (13) can be divided through by E, which then no longer influences the calculated camber. Second, if the environmental strain gradient is linear, the right side of Eq. (13) simplifies to $-EI_{tr}\alpha\Delta T/h$, where α is the coefficient of thermal expansion and ΔT is the temperature difference over the height of the girder. Then Eq. (13) reduces to Eq. (14).

$$\phi = -\frac{\alpha\Delta T}{h} \qquad (14)$$

Once ε_0 and ϕ are known, the total strain field can be calculated from Eq. (3), and the stresses from Eq. (4).

In general, the curvatures at several points along the girder must be computed and then integrated to give the camber. However, if the girder is prismatic and the thermal conditions are the same along the length, the thermal curvature will be constant along the length and may be computed at a single location. The midspan deflection is obtained by integrating this curvature twice. If the member is simply supported, the camber at midspan Δ_{camber} is given by Eq. (15).

$$\Delta_{camber} = -\frac{\phi L^2}{8} \qquad (15)$$

where

L = length of the girder

The negative sign in Eq. (15) results from the fact that the calculated deflection is negative, but in practice, camber is taken as positive upwards.

The measured temperature profiles were used to predict camber changes in girders H6B and H8A over the period that they were monitored. For simplicity, the gross (rather than the transformed) section properties were used in the calculations. According to the Federal Highway Administration, the coefficient of thermal expansion of portland cement concrete ranges from about 4.4×10^{-6} to 6.6×10^{-6}/°F (7.9×10^{-6} to 12.0×10^{-6}/°C).[12] Wight and MacGregor found that the coefficient of thermal expansion for normal-weight concretes made with siliceous aggregates ranges from 5.0×10^{-6} to 7.0×10^{-6}/°F (9.0×10^{-6} to 12.6×10^{-6}/°C).[13] In their calculations, Barr et al. assumed a value of 6.5×10^{-6}/°F (11.7×10^{-6}/°C) for this coefficient.[14]

Figure 6 compares the measured camber histories with the values calculated using Eq. (12) to (15) and the measured thermal profiles. Two calculated curves are shown, corresponding to coefficients of thermal expansion of 5.5×10^{-6} °F (9.9×10^{-6}/°C) and 6.5×10^{-6}/°F (11.7×10^{-6}/°C). The calculated and measured cambers rise and fall at similar rates and peak at similar times. The calculated curves matched the measured ones most closely when the coefficient of thermal expansion of the concrete was taken as 5.5×10^{-6}/°F. The small discrepancies can be attributed to the following:

- the assumed value for the coefficient of thermal expansion
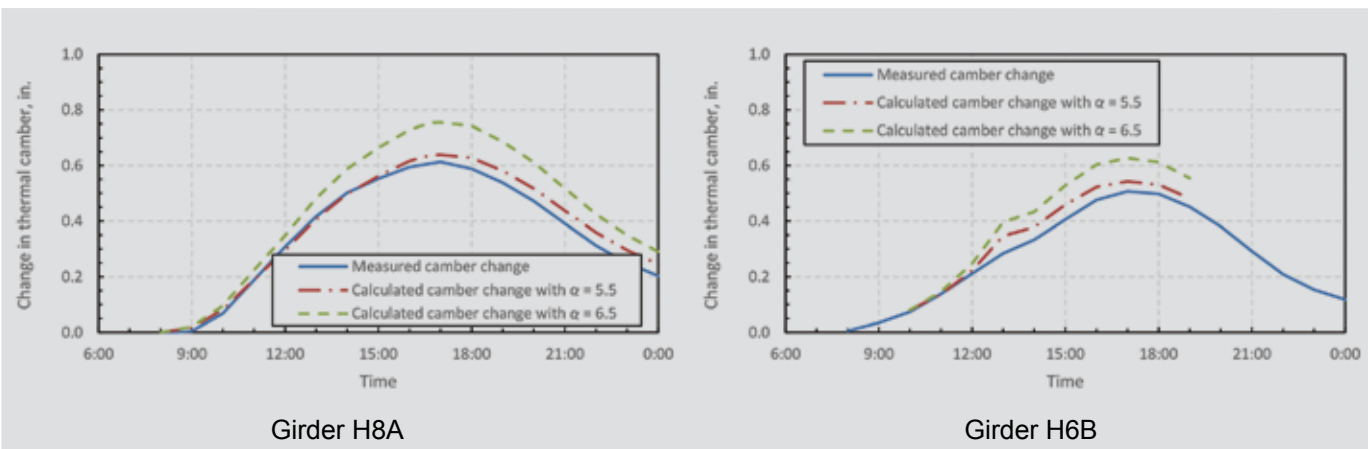
Figure 6. Comparison between calculated and measured thermal cambers. Note: α = coefficient of thermal expansion. 1 in. = 25.4 mm.

- measurement errors

- variations in *E* over the cross section

- error introduced by an insufficiently fine mesh of measured temperature data (particularly in the top flange)

Figure 6 shows that thermal cambers can be computed based on measured internal temperatures. In practice, such internal temperature data are rarely available. Therefore, two practical methods were developed to predict the thermal camber histories that require knowledge of the air temperature alone. In the following two sections, these two methods are referred to as the temperature history camber model and the peak temperature camber model.

Temperature history camber model

The temperature history camber model is based on the assumption that the temperature difference between the top and bottom of the girders can be related to variations in the ambient temperature. Site-specific data should be used when available. In their absence, the ambient temperature histories from a nearby meteorological station should be used.

Although the measured temperature data showed that the temperature profiles in the girders were highly nonlinear, the nonlinear temperature profiles nonetheless resulted in a linear total strain profile, in accordance with the Bernoulli hypothesis that plane sections remain plane. In the temperature history camber model, the total strain profile is assumed to be linear and is represented by an effective thermal strain gradient that varies linearly from zero at the bottom of the girder to an effective free thermal strain of $\varepsilon_{TH,eff}$ at the top (**Fig. 7**). For simplicity, the thermal difference that leads to $\varepsilon_{TH,eff}$ is taken to be proportional to the daily variation in ambient temperature. The constant of proportionality between $\varepsilon_{TH,eff}$ and the ambient temperature is then obtained by calibration against measured camber data.

For the effective strain profile shown in Fig. 7, the corresponding thermal curvature is Eq. (16).

$$\phi(t) = \frac{\varepsilon_{TH,eff}(t)}{h} \qquad (16)$$

where

$\phi(t)$ = curvature as a function of time

$\varepsilon_{TH,eff}(t)$ = effective free thermal strain $\alpha\Delta T_{eff}$ at time t

ΔT_{eff} = effective temperature difference between top and bottom of girder

The corresponding camber at midspan for a simply supported girder can be computed using Eq. (15).

To calculate the camber at a particular time during the day, $\Delta T_{eff}(t)$ is needed. In the temperature history camber
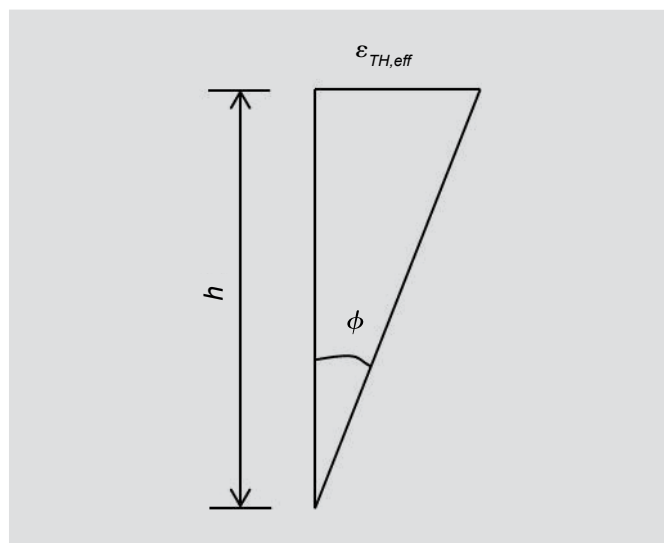
Figure 7. Effective thermal strain in girders. Note: *h* = depth of the girder; $\varepsilon_{TH,eff}(t)$ = effective thermal strain at time *t*; ϕ = curvature.

model, the effective girder temperature difference is approximated (Eq. [17]).

$$\Delta T_{eff}\left(t\right) = A_o\left[T_{amb}\left(t\right) - T_{min}\right] \qquad (17)$$

where

$T_{amb}(t)$ = ambient temperature at time t

T_{min} = minimum ambient temperature for that day

The calibration factor A_0 accounts for the differences between the ambient and girder temperatures, the actual concrete temperature profile and the effective linear one, and the actual and assumed values of α.

ΔT_{eff}, the effective difference in top and bottom concrete temperatures, is not equal to the difference in air temperature at the two locations because of the girder's thermal mass. To reflect this effect, $T_{amb}(t)$ in Eq. (17) was taken as the average of the air temperature at time t and those during the two preceding hours to give Eq. (18).

$$T_{amb,eff}\left(t\right) = \frac{T_{amb}\left(t\right) + T_{amb}\left(t-1\right) + T_{amb}\left(t-2\right)}{3} \qquad (18)$$

Substituting Eq. (16) and (17) into Eq. (15), leads to a simple equation for estimating the thermal camber change for a simply supported prismatic girder.

$$\Delta_{camber} = \frac{\alpha A_0}{h}\left[T_{amb,eff}\left(t\right) - T_{min}\right]\frac{L^2}{8} \qquad (19)$$

where

$T_{amb,eff}(t)$ = effective ambient temperature at time t

A_0 = calibration factor

The value of A_0 was determined by calibrating Eq. (19) to best reproduce 164 observations of 24 girders (on 7 different days) located in three states. They included data from the 2 girders from this study, 5 girders from Barr,[6] 14 from French and O'Neill,[9] and 3 from Hinkle.[8] All of those girders had I-shaped cross sections, but they had a variety of depths, lengths, times of casting and times of measurement. **Table 2** summarizes their key properties. **Table 3** summarizes the thermal camber data and the related meteorological information on the measurement dates.

The measured camber values M_i were compared with the calculated camber values C_i that were obtained using

Eq. (19). The root mean square camber error over time was defined using Eq. (20).

$$Error_{rms} = \sqrt{\sum_{i=1}^{n}\frac{\left(M_i - C_i\right)^2}{n}} \qquad (20)$$

The parameter A_0 in Eq. (19) was optimized to minimize the root mean square error assuming a coefficient of thermal expansion α equal to $5.5 \times 10^{-6}/°F$ ($9.9 \times 10^{-6}/°C$). **Figure 8** shows the value of A_0 optimized for each girder individually. A value of A_0 of 1.31 gave the optimum fit for the girder population, resulting in root mean square camber error over all girders of 0.11 in. (2.8 mm).

Figure 9 compares the measured thermal camber histories with those predicted by the temperature history camber model (A_0 equal to 1.31) for the seven Washington girders. The calculated and measured values are represented, respectively, by continuous and dashed lines. The occurrence of several dashed lines in a single plot indicates that the cambers of several nominally identical girders were measured on the same day, so the calculated cambers are the same.

The temperature history camber model reproduced the camber histories well for girders 1A, 1C, 2A, 2B, 2C. The discrepancy between the peak calculated and measured cambers was never more than about 0.15 in. (3.8 mm). The peak discrepancies were greater for girder H6B (0.30 in. [7.6 mm]). One possible explanation for the larger discrepancy for girder H6B is that one side of this girder was exposed to sunlight. Therefore, the girder was heated over its whole height, whereas the other girders were subjected to solar radiation primarily on the top flange. The more uniform temperature gradient of girder H6B should lead to a smaller camber. Another contributing factor is that the Washington girders were wide-flange (WF100G) sections, whereas the five girders from Barr had standard flanges (W74G sections).[6] The WF series have larger top flanges that will tend to heat up more slowly in the same ambient temperature change than a girder with a thinner flange.

Figure 10 compares the measured and calculated thermal cambers using the temperature history camber model (A_0 equal to 1.31) for the Minnesota and Georgia girders. The cambers predicted by the temperature history camber model were close to the measured values for all of the Minnesota girders. However, the errors were larger for the Georgia girders, for which the environmental conditions (for example, temperature, humidity, and length of day) may have differed from those in Washington and Minnesota.

Peak temperature camber model

A second, simpler model, called the peak temperature camber model, was developed. This method does not

Girder	Girder mark	Girder type	Location	Depth, in.	Length, ft	Length/depth
1	1A	W74MG	Washington	74	80	13.0
2	1C	W74MG	Washington	74	80	13.0
3	2A	W74MG	Washington	74	137	22.2
4	2B	W74MG	Washington	74	137	22.2
5	2C	W74MG	Washington	74	137	22.2
6	H6B	WF100G	Washington	100	173	20.7
7	H8A	WF100G	Washington	100	164	19.7
8	MN54, beam 1	MN54	Minnesota	54	122	27.1
9	MN54, beam 2	MN54	Minnesota	54	122	27.1
10	MN54, beam 3	MN54	Minnesota	54	122	27.1
11	MN54, beam 4	MN54	Minnesota	54	122	27.1
12	MN63, beam 1	MN63	Minnesota	63	132	25.1
13	MN63, beam 2	MN63	Minnesota	63	132	25.1
14	MN63, beam 3	MN63	Minnesota	63	132	25.1
15	MN63, beam 4	MN63	Minnesota	63	132	25.1
16	MN45, beam 1	MN45	Minnesota	45	119	31.7
17	MN45, beam 2	MN45	Minnesota	45	119	31.7
18	MN45, beam 3	MN45	Minnesota	45	119	31.7
19	MN45, beam 1*	MN45	Minnesota	45	119	31.7
20	MN45, beam 2*	MN45	Minnesota	45	119	31.7
21	MN45, beam 3*	MN45	Minnesota	45	119	31.7
22	W45, 6	W45	Georgia	79	129	19.6
23	W45, 7	W45	Georgia	79	128	19.5
24	W45, 8	W45	Georgia	79	127	19.3

Note: 1 in. = 25.4 mm; 1 ft = 0.305 m.
* MN45 beams 1, 2, and 3 were monitored two days (May 17, 2011, and June 30, 2011).

require a detailed daily temperature history. It is based on the assumption that the effective temperature difference between the girder top and bottom girder ΔT_{eff} is related to the daytime high temperature and the nighttime low temperature for that 24-hour period.

Proposed model

To estimate the camber at any time during the day, an instantaneous value of $\Delta T_{eff}(t)$ is needed (Eq. [14]). In the peak temperature camber model described here, that effective temperature is approximated from the maximum and minimum air temperatures of that day using a cosine interpolation function that is a function of time (Eq. [21]):

$$\Delta T_{eff}\left(t\right) = A_1\left(T_{max} - T_{min}\right)\frac{\left\{1-\cos\left[\frac{\left(t-t_0\right)}{24}\left(2\pi\right)\right]\right\}}{2} \quad (21)$$

where

t_0 = reference time for counting the thermal camber during that day

T_{max} = maximum air temperature during the 24-hour period

T_{min} = minimum air temperature during the 24-hour period

Table 3. Summary of measured data

Girder	Measurement date	Meteorological station	T_{min}, °F	T_{max}, °F	Number of observations	Maximum measured thermal camber, in.
1	June 5, 1997	Covington, Wash.	48	65	7	0.10
2	June 5, 1997	Covington, Wash.	48	65	7	0.14
3	June 5, 1997	Covington, Wash.	48	65	7	0.38
4	June 5, 1997	Covington, Wash.	48	65	7	0.37
5	June 5, 1997	Covington, Wash.	48	65	7	0.42
6	July 26, 2012	Tacoma, Wash.	55	76	18	0.51
7	July 25, 2012	Tacoma, Wash.	54	76	18	0.61
8	September 28, 2010	Elk River, Minn.	50	62	7	0.34
9	September 28, 2010	Elk River, Minn.	50	62	7	0.32
10	September 28, 2010	Elk River, Minn.	50	62	7	0.30
11	September 28, 2010	Elk River, Minn.	50	62	7	0.30
12	May 17, 2011	Elk River, Minn.	44	67	5	0.73
13	May 17, 2011	Elk River, Minn.	44	67	5	0.64
14	May 17, 2011	Elk River, Minn.	44	67	5	0.77
15	May 17, 2011	Elk River, Minn.	44	67	5	0.59
16	May 17, 2011	Elk River, Minn.	44	67	5	1.06
17	May 17, 2011	Elk River, Minn.	44	67	5	0.95
18	May 17, 2011	Elk River, Minn.	44	67	5	0.83
19	June 30, 2011	Elk River, Minn.	73	92	7	1.02
20	June 30, 2011	Elk River, Minn.	73	92	7	0.83
21	June 30, 2011	Elk River, Minn.	73	92	7	0.71
22	August 25, 2003	Savannah Airport, Ga.	74	90	3	0.50
23	August 25, 2003	Savannah Airport, Ga.	74	90	3	0.32
24	August 25, 2003	Savannah Airport, Ga.	74	90	3	0.46

Note: T_{max} = maximum temperature during a day; T_{min} = minimum temperature during a day. 1 in. = 25.4 mm; °C = (°F − 32)/1.8.
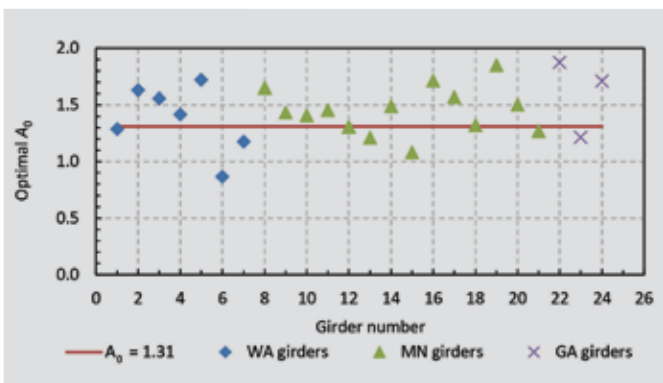

**Figure 8.** Optimized values of calibration factor A_0 of all girders.

The time offset t_0 reflects several influences, including the time at which the ambient temperature is at a minimum and the lag between the concrete and air temperatures. Then ΔT_{eff} has the value of zero when t equals t_0 (or t_0 + 24 hours) and reaches its maximum of $A_1(T_{max} - T_{min})$ at t equal t_0 + 12 hours, where A_1 is a calibration factor.

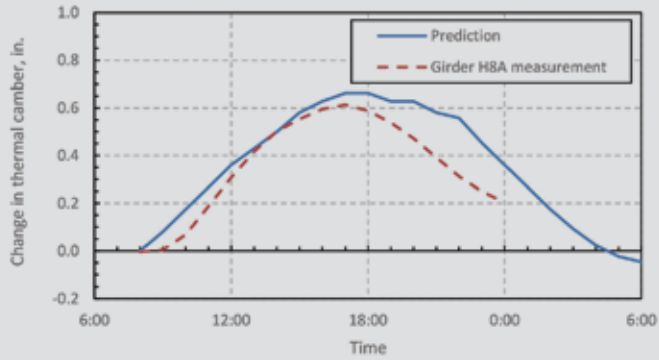The effective thermal strain is calculated using Eq. (22).

$$\varepsilon_{TH,eff} = \alpha A_1 \left(T_{max} - T_{min} \right) \frac{\left\{ 1 - \cos\left[\frac{(t - t_0)}{24}(2\pi) \right] \right\}}{2} \quad (22)$$
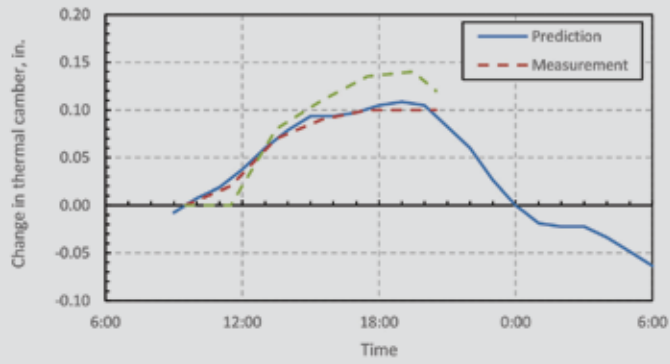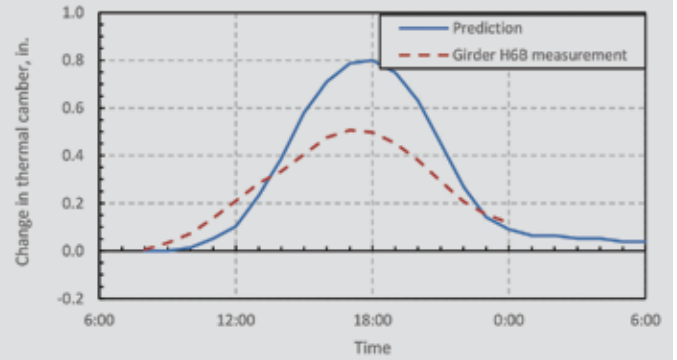
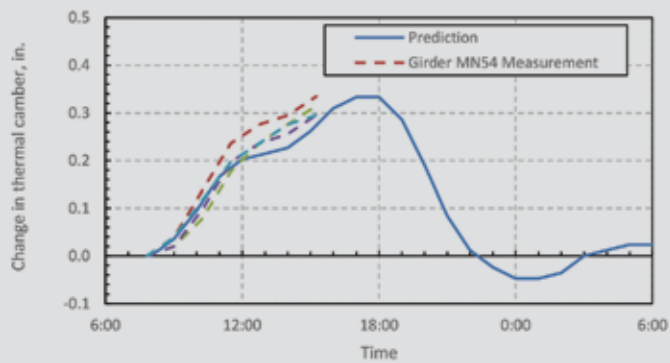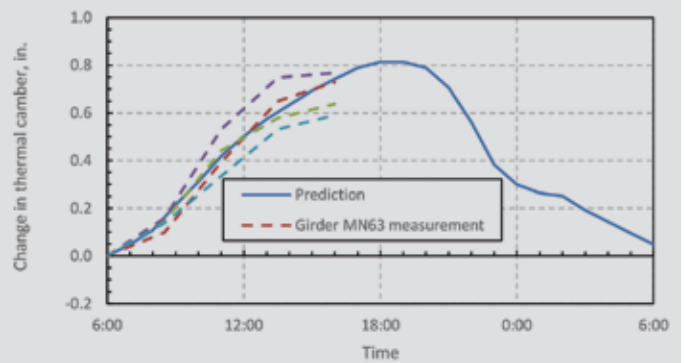Girders 1A and 1C
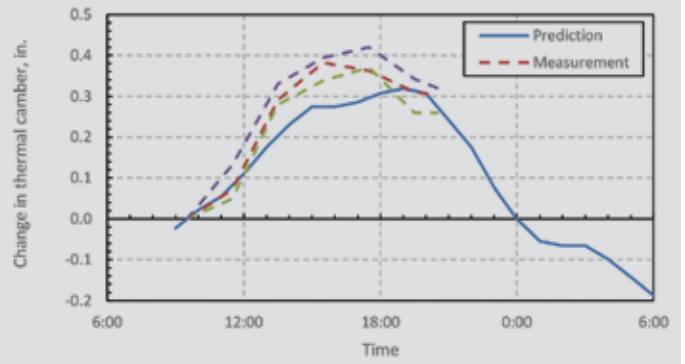
Girders 2A, 2B, and 2C
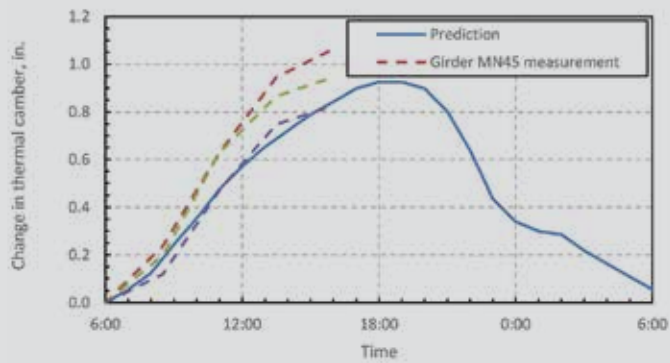
Girder H8A

Girder H6B

Figure 9. Temperature history camber model: comparison of measured and calculated thermal camber changes in Washington State girders. Note: 1 in. = 25.4 mm.
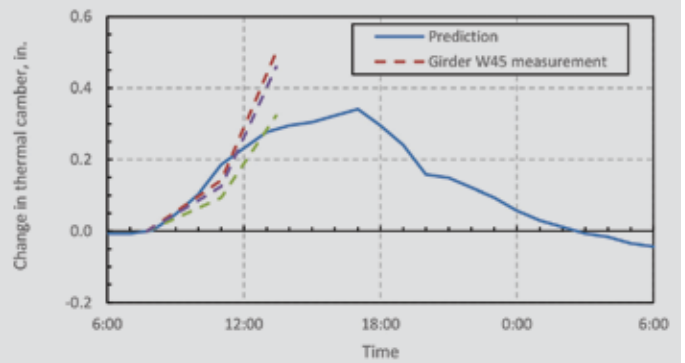

MN54 girders

MN63 girders

MN45 girders (measured on May 17, 2011)

W45 girders, Georgia

Figure 10. Temperature history camber model: comparison of measured and calculated thermal camber changes for Minnesota and Georgia State girders. Note: 1 in. = 25.4 mm.

Combining Eq. (15) and (22) results in Eq. [23], which gives the thermal camber at midspan for a simply supported girder.

$$\Delta_{camber} = \left(\frac{\alpha A_1}{h}\right)\left(\frac{(T_{max} - T_{min})\left\{1 - \cos\left[\frac{(t - t_0)}{24}(2\pi)\right]\right\}}{2}\right)\left(\frac{L^2}{8}\right) \quad (23)$$

Calibration of peak temperature camber model

As was done for the temperature history camber model, the peak temperature camber model was calibrated by optimizing predictions of the cambers. **Table 4** lists the optimal model parameters and individual root mean square errors in Eq. (20) when each of the 24 girders was considered individually. The model was then optimized against the data from all girders at once, and the values A_1 of 1.28 and t_0 of 4.53 (rounded to 4.5) were found to be optimal, with a root mean square camber error of 0.09 in. (2.3 mm).

Figure 11 compares the measured and calculated thermal camber changes using the peak temperature model with A_1 of 1.28 and t_0 of 4.5 for the Washington girders. As was the case with the temperature history camber model, the greatest error occurred in girder H6B of Washington (0.20 in. [5 mm]). As discussed previously, girder H6B was unusual in that its left side was exposed to the sun. Neither the temperature history camber model nor the peak temperature camber model considered this factor.

Figure 12 compares the measured and calculated cambers for the Minnesota and Georgia girders. The peak temperature model works well for Minnesota girders. The shapes of the measured and calculated curves were similar, and the average error was less than 0.1 in. (2.5 mm). As was the case in the temperature history camber model, the measured and predicted cambers differed more for the Georgia girders.

Conclusion

This research leads to the following conclusions:

- The temperature profile in a precast concrete girder can be highly nonlinear during the afternoon, with a large temperature gradient within the top flange.

- The camber histories computed from the internal temperature profiles of two instrumented girders were close to the measured values. This finding not only verifies the computational method used but it also suggests that the spatial density of measured temperature readings was sufficient for that purpose.

Table 4. Root mean square errors between measured and calculated thermal camber changes using variables of A_1 and t_0

Girder	Girder mark	Location	Optimum A_1	Optimum t_0	Error, in.
1	1A	Washington	1.11	5.80	0.006
2	1C	Washington	1.05	6.98	0.014
3	2A	Washington	1.25	5.21	0.033
4	2B	Washington	1.19	5.00	0.039
5	2C	Washington	1.44	5.01	0.018
6	H6B	Washington	0.78	4.51	0.045
7	H8A	Washington	1.20	5.53	0.040
8	MN54, beam 1	Minnesota	1.46	3.35	0.019
9	MN54, beam 2	Minnesota	1.20	5.13	0.020
10	MN54, beam 3	Minnesota	1.19	4.04	0.021
11	MN54, beam 4	Minnesota	1.26	3.64	0.011
12	MN63, beam 1	Minnesota	1.24	4.90	0.032
13	MN63, beam 2	Minnesota	1.12	3.68	0.025
14	MN63, beam 3	Minnesota	1.38	3.70	0.041
15	MN63, beam 4	Minnesota	1.00	4.30	0.009
16	MN45, beam 1	Minnesota	1.58	4.23	0.016
17	MN45, beam 2	Minnesota	1.45	3.88	0.038
18	MN45, beam 3	Minnesota	1.24	4.68	0.039
19	MN45, beam 1	Minnesota	1.72	4.24	0.059
20	MN45, beam 2	Minnesota	1.40	4.32	0.048
21	MN45, beam 3	Minnesota	1.18	4.62	0.052
22	W45, 6	Georgia	3.96	8.23	0.000
23	W45, 7	Georgia	2.52	8.19	0.000
24	W45, 8	Georgia	3.71	8.28	0.000

Note: A_1 = calibration factor; t_0 = reference time for counting thermal camber during a day.

- Both the temperature history camber model and the peak temperature camber model had root mean square average camber errors over time of about 0.1 in. (2.5 mm) when applied to a range of girders, all with I-shaped cross sections. Such small errors would not significantly affect the installation of girders onsite. Since the peak temperature camber model is simpler than the temperature history camber model (and for these data, slightly more accurate), the peak temperature camber model is recommended for practice for use with I-shaped girders on simple spans. It has not
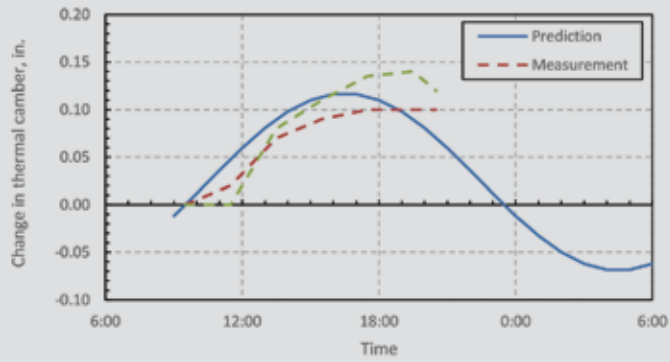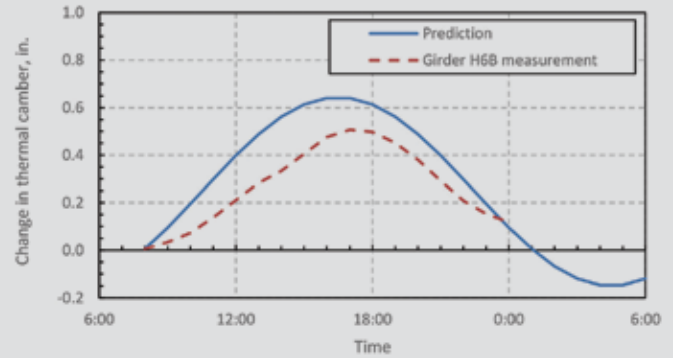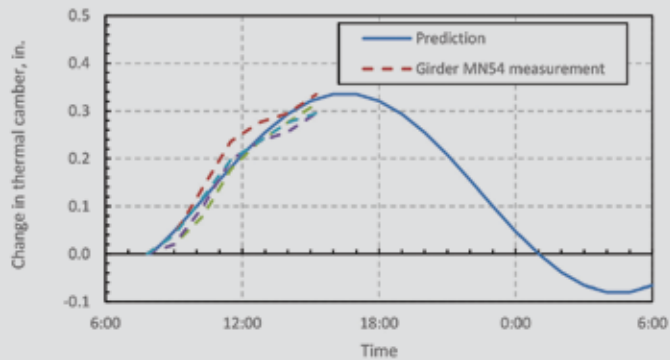
Girders 1A and 1C
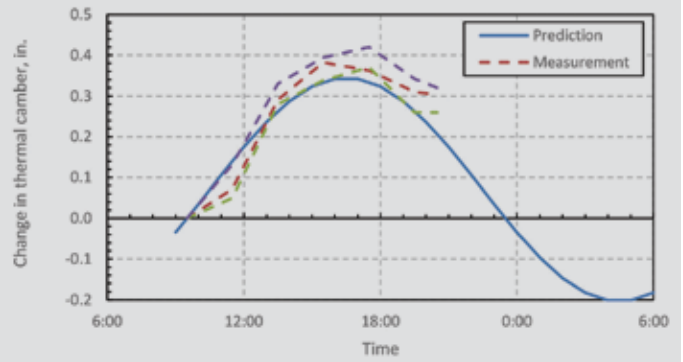
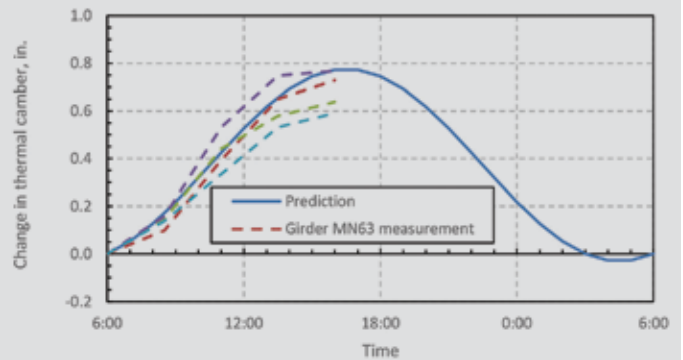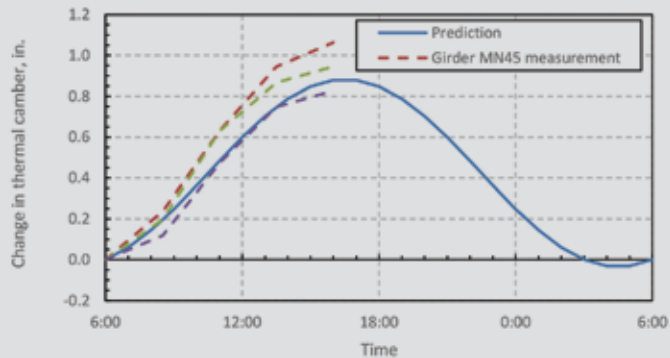Girders 2A, 2B, and 2C
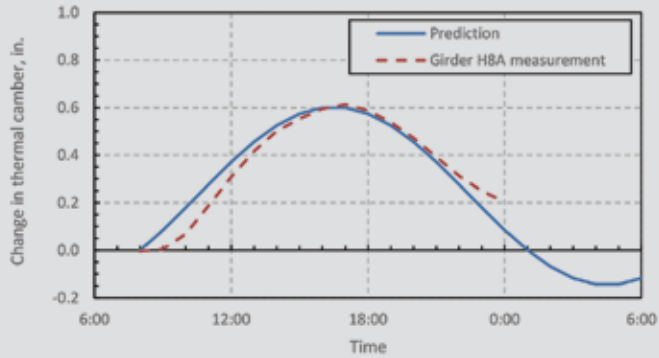
Girder H8A

Girder H6B

Figure 11. Peak temperature camber model: comparison of measured and calculated thermal camber changes for Washington State girders. Note: 1 in. = 25.4 mm.
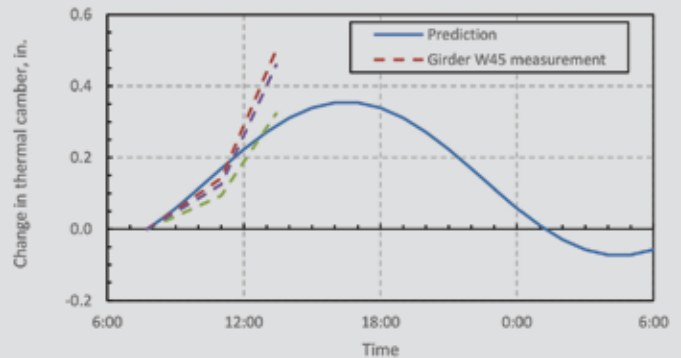

MN54 girders

MN63 girders

MN45 girders (measured on May 17, 2011)

W45 girders, Georgia

Figure 12. Peak temperature camber model: comparison of measured and calculated thermal camber changes for Minnesota and Georgia State girders. Note: 1 in. = 25.4 mm.

been calibrated with other cross-sectional shapes or other boundary conditions.

- The accuracy of the camber prediction depended on the details of the girder's exposure to the sun. For example, the methods worked less well for Washington girder H6B, which had one side, as well as its top flange, exposed to sunlight. The models also worked better for the Washington and Minnesota girders than for the girders located in Georgia. It is possible that the differences in accuracy arise from differences in temperature, humidity, or solar radiation conditions. It is also possible that the discrepancies are attributable to the paucity of camber observations for the Georgia girders.

References

1. Tadros, M. K., F. Fawzy, and K. Hanna. 2011. "Precast, Prestressed Girder Camber Variability." *PCI Journal* 56 (1): 135–154.

2. Storm, T. K., Rizkalla, S. H. and Zia, P. Z. 2013. "Effects of Production Practices on Camber of Prestressed Concrete Bridge Girders." *PCI Journal* 58 (1): 96–111.

3. AASHTO (American Association of State Highway and Transportation Officials). 2012. *AASHTO LRFD Bridge Design Specifications*. 6th ed. Washington, DC: AASHTO.

4. Priestley, M. J. N. 1978. "Design of Concrete Bridge for Temperature Gradients." *ACI Journal* 75 (5): 209–217.

5. Shushkewich, K. W. 1998. "Design of Segmental Bridge for Thermal Gradient." *PCI Journal* 43 (4): 120–137.

6. Barr, P. J. 2000. "Consistent Crudeness in Prestressed Concrete Girder Design." PhD diss., University of Washington, Seattle, WA.

7. AASHTO. 1994. *AASHTO LRFD Bridge Design Specifications*. 1st ed. Washington, DC: AASHTO.

8. Hinkle, S. D. 2006. "Investigation of Time-Dependent Deflection in Long Span, High Strength, Prestressed Concrete Bridge Beams" MSCE thesis, Virginia Polytechnic Institute and State University, Blacksburg, VA.

9. French, C. E., and C. R. O'Neill. 2012. "Validation of Prestressed Concrete I-Beam Deflection and Camber Estimates." MnDOT (Minnesota Department of Transportation) final report 2012-16, MnDOT Research Service, St. Paul, MN.

10. Nguyen, H. 2014. "Improving Predictions for Camber in Precast, Prestressed Concrete Bridge Girders." MSCE thesis. University of Washington, Seattle, WA.

11. Washington State Department of Transportation. 2015. *Bridge Design Manual* (LRFD). http://www.wsdot.wa.gov/Publications/Manuals/M23-50.htm.

12. Federal Highway Administration. 2011. "Portland Cement Concrete Pavements Research." http://www.fhwa.dot.gov/publications/research/infrastructure/pavements/pccp/thermal.cfm.

13. Wight, J. K., and J. G. MacGregor, 2012. "Reinforced Concrete Mechanics and Design." 6th ed. Upper Saddle River, NJ: Pearson Education Inc.

14. Barr, P. J., Stanton, J. F., and M. O. Eberhard. 2005. "Effects of Temperature Variations on Precast, Prestressed Concrete Bridge Girders." *ASCE Journal of Bridge Engineering* 10 (2): 186–194.

Notation

A_0 = calibration factor

A_1 = calibration factor

A_{tr} = area of the transformed section

$b(y)$ = girder width

C_i = computed camber values

E = Young's modulus

$Error_{rms}$ = root mean square camber error over time of a girder

f_c' = compressive strength of concrete

h = depth of the girder

h_a = asphalt thickness

I_{tr} = moment of inertia of the transformed section

L = length of the girder

M_i = measured camber values

t = time

t_0 = reference time for counting thermal camber during a day

$t(Y)$ = change in temperature at height Y

T = temperature at top surface of deck

$T_{amb}(t)$ = ambient temperature at time t

$T_{amb,eff}(t)$ = effective ambient temperature at time t

T_{max} = maximum temperature during a day

T_{min} = minimum temperature during a day

y = vertical coordinate, measured positive downwards from origin

Y = vertical coordinate, measured upwards from a point located Y_0 below the concrete deck surface

Y_0 = distance from top surface at which temperature change is zero

α = coefficient of thermal expansion

Δ_{camber} = camber of girder

ΔT = temperature difference over the height of the girder

ΔT_1 = temperature change at top surface of girder in AASHTO LRFD specifications profile

ΔT_2 = temperature change 4 in. (100 mm) below top surface of girder in AASHTO LRFD specifications profile

ΔT_3 = temperature change at bottom of girder in AASHTO LRFD specifications profile

ΔT_{eff} = effective temperature difference between top and bottom of girder

$\Delta T_{eff}(t)$ = instantaneous effective temperature difference between top and bottom of girder

ε_0 = total strain at origin

ε_e = free environmental strain

ε_m = mechanical strain

ε_{tot} = total strain

$\varepsilon_{TH,eff}$ = effective thermal strain

$\varepsilon_{TH,eff}(t)$ = effective thermal strain at time t

σ = stress

ϕ = curvature

$\phi(t)$ = curvature as a function of time

About the authors

Hang Nguyet Nguyen is a research associate at Nanyang Technological Institute in Singapore, where she is enrolled in the PhD program. She received her MSCE from the University of Washington in Seattle, Wash., where she conducted research on camber in prestressed concrete girders.

David D. Chapman, PE, is chief engineer for Concrete Technology Corp. in Tacoma, Wash. He is a member of the PCI Committee on Bridges and has more than 14 years of experience in the design and manufacture of prestressed concrete members.

Marc O. Eberhard, PhD, is a professor at the University of Washington. He received his BSCE degree from the University of California, Berkeley, in 1984, and he received his MSCE and PhD degrees from the University of Illinois at Urbana-Champaign in 1987 and 1989. Along with his colleagues, he received the PCI Charles Z. Zollman Award in 2013.

John Stanton, PhD, PE, is a professor of civil engineering at the University of Washington. He holds degrees from the University of Cambridge in the United Kingdom, Cornell University in Ithaca, N.Y., and University of California, Berkeley, and has worked in practice in England, France, and Canada. His research interests lie in prestressed and precast concrete, and he has concentrated recently on accelerated bridge construction.

Abstract

It is important to estimate girder camber accurately because differences between expected and actual camber can lead to construction challenges or girder rejection. Field measurements of daily variations in temperature profile and camber for two precast, prestressed concrete girders provided data with which to calibrate models of the effect of temperature variations on camber. Using measured temperature profiles over the height of the girder, the associated camber history was accurately computed, assuming a coefficient of thermal expansion of $5.5 \times 10^{-6}/°F$ ($9.9 \times 10^{-6}/C$). Two practical methods were also developed using 164 observations from 24 girders. To implement the simpler method (peak temperature camber method), the designer needs only to know the girder's length and depth and to estimate the maximum change in air temperature during the day, which is available from meteorological stations. The errors in the resulting models had root mean square average camber over time of about 0.1 in. (2.5 mm).

Keywords

Bridge, camber, girder, temperature.

Review policy

This paper was reviewed in accordance with the Precast/Prestressed Concrete Institute's peer-review process.

Reader comments

Please address reader comments to journal@pci.org or Precast/Prestressed Concrete Institute, c/o *PCI Journal*, 200 W. Adams St., Suite 2100, Chicago, IL 60606. ∏